In Situ Synthesis of Polyamide 6/MWNTs Nanocomposites by Anionic Ring Opening Polymerization

Dongguang Yan,[1,2] Tingxiu Xie,[3] Guisheng Yang[1,3]

[1]*CAS Key Laboratory of Engineering Plastics, Joint Laboratory of Polymer Science and Materials, Institute of Chemistry, The Chinese Academy of Sciences, Beijing 100080, People's Republic of China*
[2]*Graduate School of the Chinese Academy of Sciences, Beijing 100039, People's Republic of China*
[3]*Shanghai Genius Advanced Materials Co. Ltd., Shanghai, 201109, People's Republic of China*

Received 24 February 2008; accepted 27 July 2008
DOI 10.1002/app.29005
Published online 22 October 2008 in Wiley InterScience (www.interscience.wiley.com).

ABSTRACT: *In situ* anionic ring opening polymerization is used to prepare monomer casting polyamide 6 (MCPA6)/carbon nanotubes (CNTs) nanocomposites, whereby water is used as auxiliary dispersing agent of hydroxyl functionalized multiwalled carbon nanotubes (MWNTs-OH) and ε-caprolactam (CL) monomer. The MWNTs-OH were dispersed homogenously in MCPA6 matrix when being observed through transmission electron microcopy. The well dispersed MWNTs-OH existed at the center of many radial texture phases in MCPA6 matrix. Polarizing microscope analysis showed that these radial texture phases were MCPA6 spherulitic crystallities. Differential scanning calorimetry analysis revealed that the crystallization temperature of the MCPA6/MWNTs-OH nanocomposites had been improved by adding only 0.2 wt % MWNTs-OH when compared with pure MCPA6. The influence of MWNTs-OH on the thermal stability of MCPA6 under nitrogen and air environments was also investigated by thermal gravimetric analysis (TGA). © 2008 Wiley Periodicals, Inc. J Appl Polym Sci 111: 1278–1285, 2009

Key words: carbon nanotubes; polyamides; nanocomposites; *in situ* polymerization; anionic ring opening

INTRODUCTION

Carbon nanotubes (CNTs) have been discovered in 1991 and can be classified into two types: single-walled carbon nanotubes (SWNTs) and multiwalled carbon nanotubes (MWNTs). MWNTs comprise concentric SWNTs held together by weak van der Waals's forces. Because of their unusual mechanical, thermal, and electrical properties, studies of polymer/CNTs composites are rapidly expanding in commercial and research labs around the world. There are three main approaches to prepare the polymer/CNTs nanocomposites: (a) melt extrusion,[1–4] (b) *in situ* polymerization,[5–9] and (c) solution mixing.[10–14] However, CNTs are strongly affected by van der Waal's forces, which give rise to the formation of aggregates, consequently making their dispersion in polymers difficult. To prepare polymer/CNTs nanocomposites with high performance, the good dispersion of CNTs in the matrix is thought to be necessary.[15–18] For this aim, functionalization or modification of CNTs become the primary focus of many research groups. A primary way is to introduce various oxygen-containing defect sites on the nanotube surface and ends. For example, by simply refluxing CNTs with nitric acid or mixed acids, some functional groups, such as carboxylic, carbonyl, and hydroxyl groups, can be introduced on CNTs.[10] These oxygenated defect sites can interact with the group of some polymer matrix via hydrogen bonding and an improved dispersion of CNTs in these matrices can be realized successfully. MWNTs only being primarily carboxylated or hydroxylated have been widely used to prepare nanocomposites.[19–23]

Polyamide 6 (PA6) is an important thermoplastic with a wide range of engineering applications, which is often reinforced with different nanofillers in practice. PA6/MWNTs-COOH nanocomposites have been successfully prepared via melt compounding or *in situ* hydrolytic polymerization.[1,2,11,20–23] However, there are few reports for the preparation of monomer casting polyamide 6 (MCPA6)/MWNTs nanocomposites via *in situ* anionic ring opening polymerization.

Raw MWNTs and MWNTs-COOH are not suitable for the preparation of MCPA6/MWNTs nanocomposites via *in situ* anionic ring opening polymerization. The dispersion of raw MWNTs in CL monomer is difficult for the weakly hydrogen bonding interaction. The carboxyl group of MWNTs-COOH usually has a severe inhibiting role on

Correspondence to: G. Yang (ygs@geniuscn.com).

anionic ring opening polymerization. In this work, hydroxyl functionalized multiwalled carbon nanotubes (MWNTs-OH) was chosen as the nanofiller to prepare MCPA6/MWNTs nanocomposites via *in situ* anionic ring opening polymerization. To improve the dispersion of MWNTs-OH in ε-caprolactam (CL) monomer, water was used as an auxiliary dispersing agent. Meanwhile, the effects of MWNTs-OH on the crystallization and thermal stability of MCPA6 were also investigated.

EXPERIMENTAL

Materials

Commercial grade ε-caprolactam was obtained from Nanjing Oriental Chemical Company and dried in vacuum at 140°C for 20 min to remove traces of water before use. MWNTs-OH (0.71 wt %OH) were purchased from Chengdu Organic Chemistry (purity > 95%, diameter > 50 nm, length 0.5–2 μm). A ε-caprolactam sodium salt (CLNa, Bruggolen C10) was received from Brüggemann Chemicals, and acted as the catalyst for anionic ring opening polymerization. Bruggolen C10 is a blend of ε-caprolactam and CLNa. The concentration of CLNa limits in 17–19 wt %. Toluene-2, 4-diisocyanate (TDI) is purchased from Shanghai Chemical Reagent Corp and was used as the activator.

Dispersion of MWNTs-OH in ε-caprolactam

A desired amount of MWNTs-OH were added to a solution of 80 g ε-caprolactam dissolved in 20 g deionized water under stiring, and a stable liquid mixture was obtained with the aid of power ultrasonic wave for 1 h. Afterwards, the mixture was firstly vacuumed at 85°C for about 1 h to remove most of the water, and then vacuumed at 170°C for 20 min to remove the trace water.

The preparation of MCPA6/MWNTs-OH nanocomposites

CLNa was added into the mixture above. Then TDI was also added into the mixture. After fully stirring, the final mixture was then immediately poured into a mold preheated to 160°C and polymerized in the oven at 160°C for 10 min. The resulted product were cooled to room temperature slowly and extracted with boiling water to eliminate the residual monomer (the equilibrium conversion is about 94–96%). Finally, MCPA6/MWNTs-OH nanocomposites with various amounts of MWNTs-OH (0.05 wt %, 0.1 wt %, and 0.2 wt %) were obtained. The treatment processes of all compositions were identical to ensure comparability and accuracy of the testing results.

Characterization

Transmission electronic microscopy

Transmission electronic microscopy (TEM) was carried out on a Hitachi H-800 microscope at an acceleration voltage of 100 kV. The samples were ultramicrotomed with a diamond knife on a Leica Ultracut UCT microtomed at −20°C to give 70 nm thick sections. The sections were transferred to carbon-coated Cu grids of 200 meshes. The contrast between the MWNTs-OH and the polymer phase was sufficient for imaging analysis, so no heavy metal staining of sections before imaging was required.

Crystallization properties

Differential scanning calorimetery (DSC) measurements were carried out on a NETZSCH DSC 200 PC calibrated using standards. All the measurements were performed from room temperature to 280°C at a heating rate of 10°C min^{-1} under a nitrogen atmosphere and held at that temperature for 5 min to erase any previous thermal history and then cooled to 50°C at a rate of 10°C/min. The second heating and cooling processes were recorded.

Polarizing optical microscopy (POM)

The semithin sections prepared by a LBK-5 ultramicrotome for polarizing optical microscopy (POM) were measured on Olympus BX51-P at room temperature.

Thermal gravimetric analysis

Thermal gravimetric analysis (TGA) was carried out using a SDT Q600 (TA Instrument Corp.) at a heating rate of 20°C/min up to 800°C under nitrogen and air flow, respectively.

RESULTS AND DISCUSSION

Dispersion of MWNTs-OH in MCPA6 martrix

The dispersion stability of nanofiller in the monomer plays an important role in the preparation of nanocomposites via *in situ* polymerization. The dispersion of raw MWNTs and MWNTs-OH in melted CL was examined firstly. The process of the dispersion was the same as that of the second section in the experiment. Figure 1 shows the digital picture of the two mixtures after being placed in an oven at 100°C for a week. It can be seen that MWNTs-OH have a better dispersion stability when compared with raw MWNTs. These differences could be attributed to the hydrogen-bonding effect. The hydroxyl groupes on the surface of MWNTs-OH interacted with the

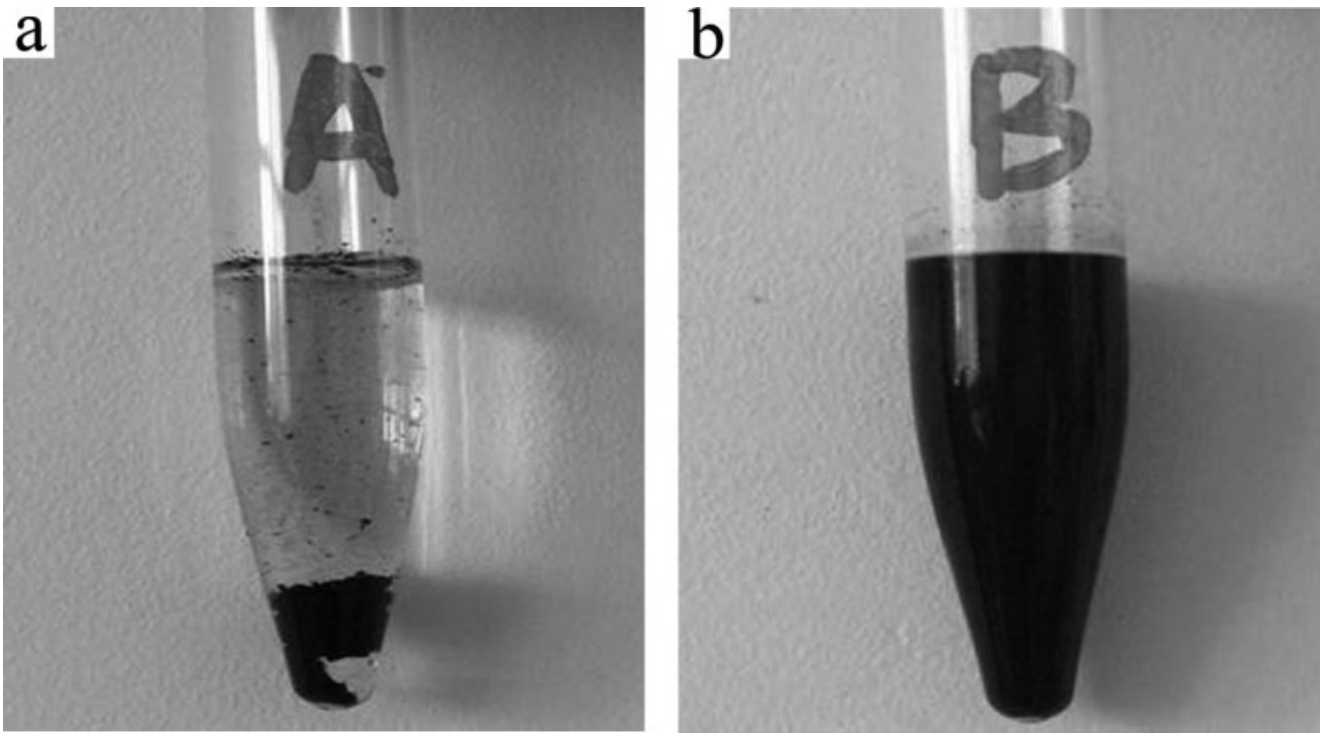

Figure 1 Dispersion stability of raw MWNTs and MWNTs-OH in melted CL after storage for a week [(a) raw MWNTs and (b) MWNTs-OH].

amine groups or the carbonyl of CL. Hydrogen-bonding interaction between MWNTs-OH and melted CL was formed. This interaction would be beneficial to the dispersion of MWNTs-OH and prevented the reagglomeration during processing. The dispersion stability of MWNTs-OH in melted CL monomer facilitated the formation of MCPA6 nanocomposites with homogenously dispersed MWNTs-OH.

The evidence of the nanometer-scale dispersion of MWNTs-OH in the polymer matrix is provided by the TEM micrographs, as shown in Figure 2. An interesting phenomenon can be found in the MCPA6/MWNTs-OH nanocomposites. There are many radial textures with black spots at their centers in the MCPA6 matrix. The quantity of the radial textures increases and the diameter of the spherulites decreases with increasing MWNTs-OH content. Such result is hardly seen in other nanocomposites with MCPA6 matrix in previous works. But similar results have been reported in some literatures about PET hybrids.[24] In those works, the radial textures in PET hybrids were proved to be with the spherulitic morphology of PET crystal, as observed by the POM images. So these radial textures in Figure 2(b–d) can also be attributed to the spherulitic morphology of MCPA6 crystals, which has been also confirmed by POM later. Many of the black spots at the centers of those radial textures in nanocomposites are some well dispersed MWNTs-OH when observed at higher magnification by TEM, as shown in Figure 2(e). These results indicate that the dispersion of MWNTs-OH in MCPA6 matrix is homogeneous. Hydrogen-bonding interaction between MWNTs-OH and MCPA6 can greatly promote the dispersion of MWNTs-OH.

Crystalline morphology

To confirm the results obtained by TEM, POM was used to study the crystalline morphology of neat MCPA6 and the MCPA6/MWNTs-OH nanocomposites. The POM images are shown in Figure 3. The crystallites of neat MCPA6 have spherulitic superstructures with distinct Maltese cross patterns from Figure 3(a). Most of the spherulites grow up to a diameter of about 20 μm. The size of the spherulites is fairly uniform, which indicates dominantly predetermined nucleation. Much higher amount of crystallites with much smaller size could be found in Figure 3(b,c). A few of the crystallites become irregularly shaped (e.g., fan-shaped crystallites). These results could be attributed to the heterogeneous nucleation of MWNTs-OH which accelerated the rate of nucleation of MCPA6 and increases the number of the crystal nucleus. The space of crystallizing was restricted. Therefore, more imperfect spherulites and microcrystals were formed for the restriction in the space.

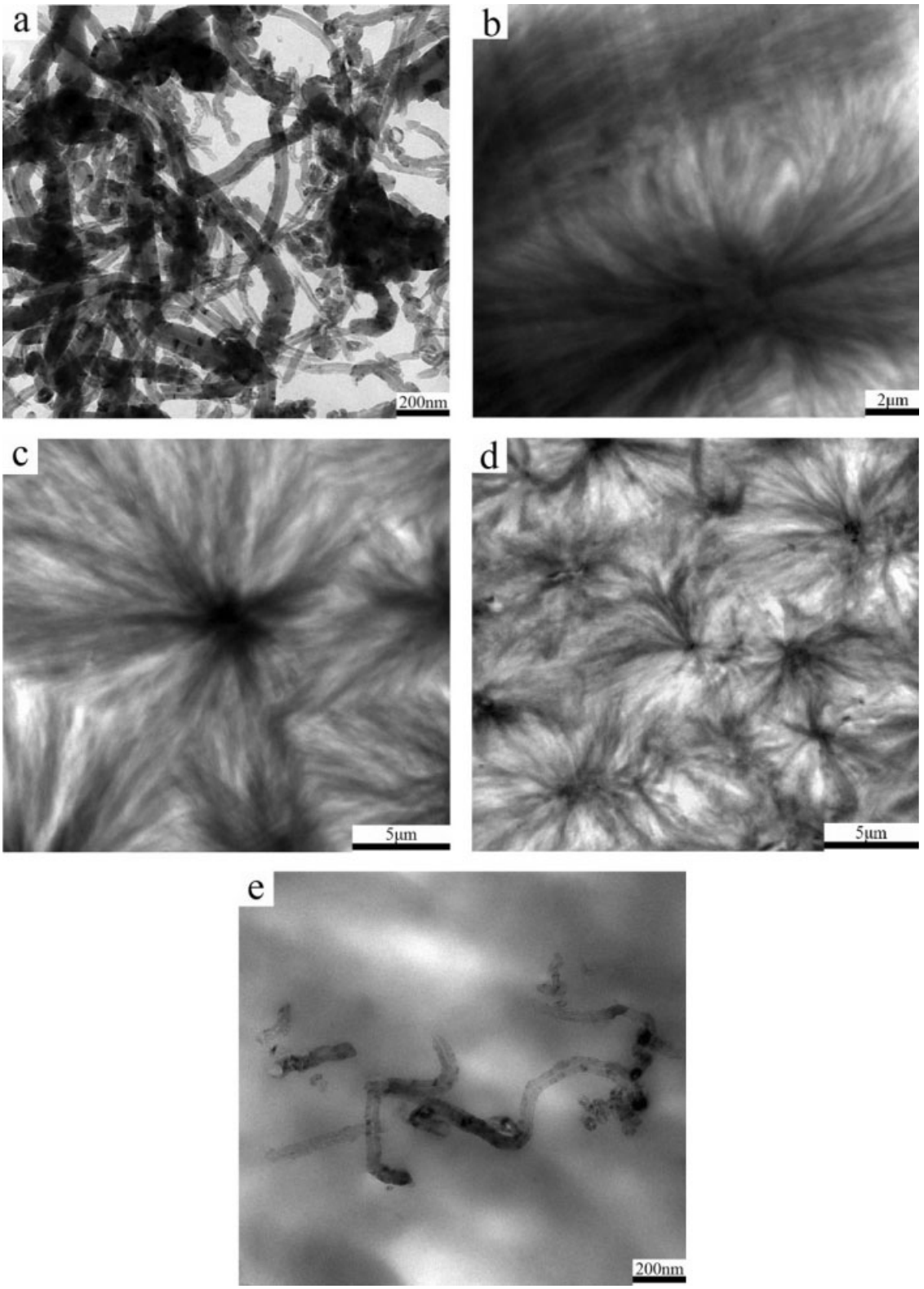

Figure 2 Representative TEM images of pure MWNTs-OH (a), pure MCPA6 (b), MCPA6/MWNTs-OH nanocomposites with 0.05 wt % (c), 0.10 wt % (d), images of nanocomposites with high magnification (e).

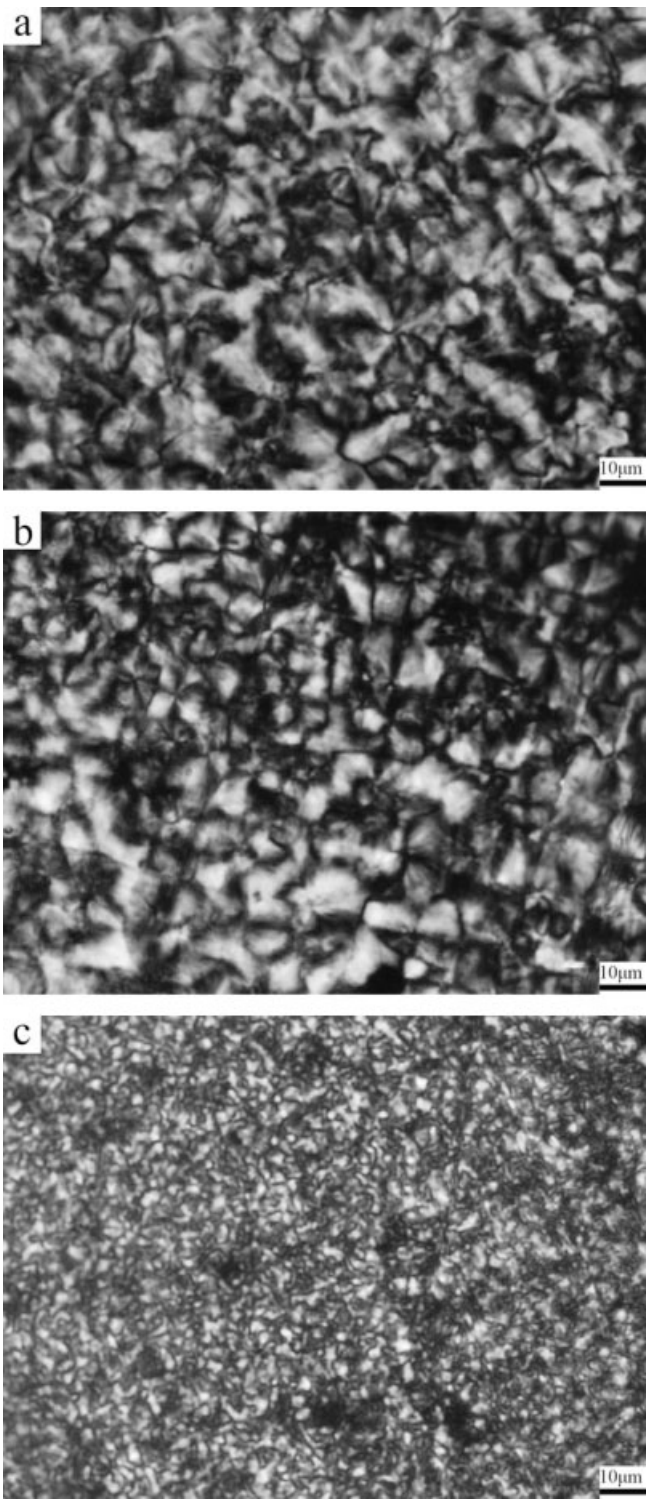

Figure 3 POM images of pure MCPA6 (a), MCPA6/MWNTs-OH nanocomposites with 0.05 wt % (b), 0.10 wt % (c).

Crystallization behavior of MCPA6/MWNT nanocomposites

The heating and cooling thermograms of neat MCPA6 and its nanocomposites with different MWNTs-OH contents are reported in Figure 4. The data are summarized in Table I in details, and the melting point (T_m) of MCPA6 has hardly been affected by MWNTs-OH. But a clear decrease of melting peak width (ΔT_m) could be found in the nanocomposites with respect to that of pure MCPA6. The value of ΔT_m for the nanocomposites with 0.2 wt % MWNTs-OH is 4°C lower than that for pure MCPA6, which indicates that the size distribution of the MCPA6 crystallites in the nanocomposites is more homogeneous than that in pure MCPA6. The crystallization temperature (T_c)of the nanocomposites is increased markedly in the cooling process, as can be seen in Figure 4(b). Table I shows that the T_c of the MCPA6/MWCNTs-OH nanocomposites with a small amount of MWCNTs-OH (0.2 wt %) is increased to 186.0°C, 7°C higher than that of neat MCPA6 (179.0°C). At the same time, it can

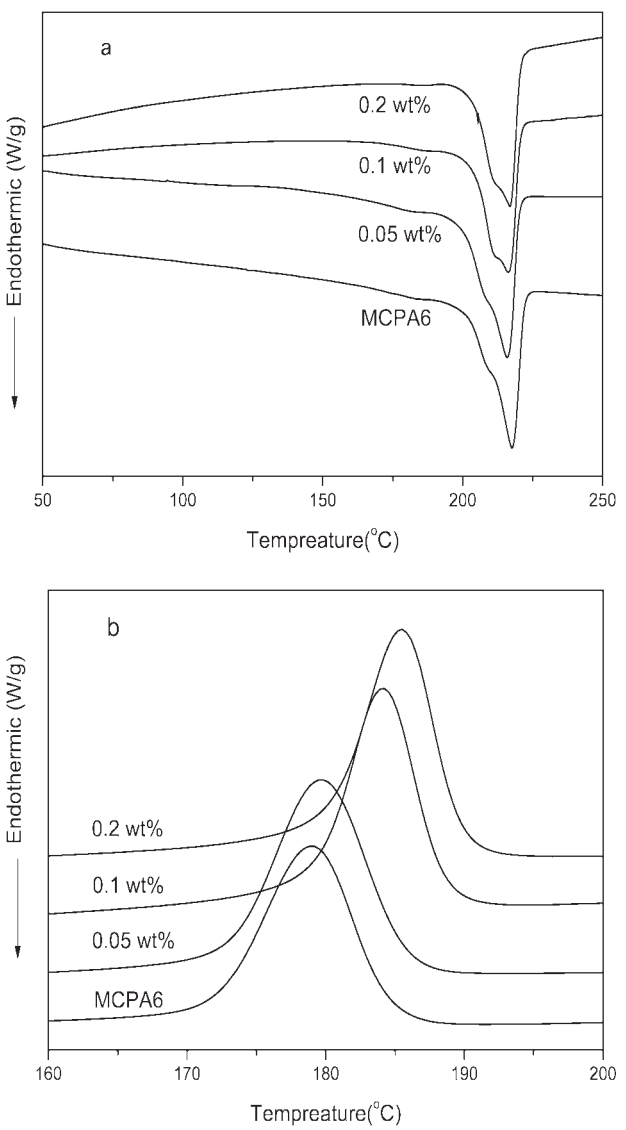

Figure 4 Thermograms of pure MCPA6 and MCPA6/MWNTs-OH with various amounts of MWNTs-OH. (a) the second heating; (b) cooling.

TABLE I
Characteristic Values of Crystallization and Melting Behavior of MCPA6 and MCPA6/MWNTs-OH Composites

MWNTs-OH content (wt %)	Heating (2nd)					Cooling		
	Onset (°C)	T_m (°C)	ΔT_m (°C)	ΔH_f (J g^{-1})	X_c (%)	ΔH_c (J g^{-1})	$T_{c,m}$ (°C)	ΔT_d (°C)
0	205	217.5	15	−65.86	28.63	56.21	179.0	38.50
0.05	205	215.7	13	−66.72	29.00	57.57	179.6	36.1
0.1	208	216.4	11	−68.84	29.93	58.78	185.0	31.4
0.2	208	216.8	11	−70.79	30.77	66.56	186.0	30.88

be seen in Table I that the degree of supercooling ($\Delta T = T_m - T_c$) of the nanocomposites decreases with respected to that of pure MCPA6. It can also been seen that the absolute degree of crystallization of MCPA6 increases slightly with increasing MWNTs content. All the above results indicate that MWNTs-OH could effectively act as nucleating agents in the PA6/MWCNT-OH nanocomposites. The incorporation of a very small quantity of MWNTs-OH into MCPA6 could therefore enhance the crystallization ability of the MCPA6 matrix through heterogeneous nucleation.

Thermal stability

Typical TGA weight loss and derivative thermograms (DTG) for MCPA6 and MCPA6/MWNTs-OH

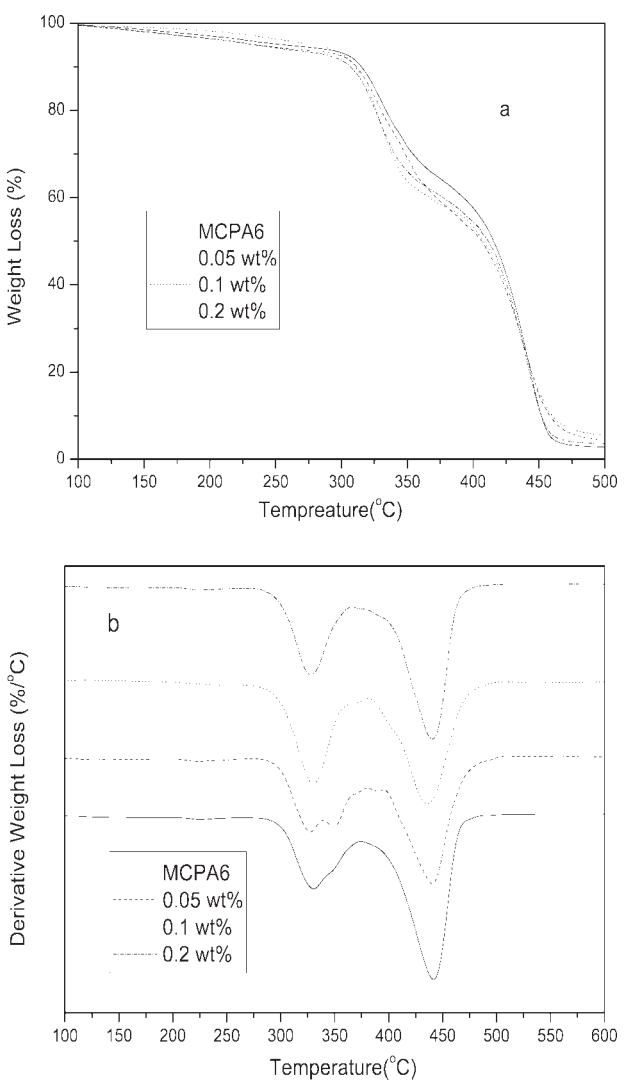

Figure 5 (a) TGA and (b) DTG curves of pure MCPA6 and MCPA6/MWNTs-OH with various amounts of MWNTs-OH under nitrogen environment.

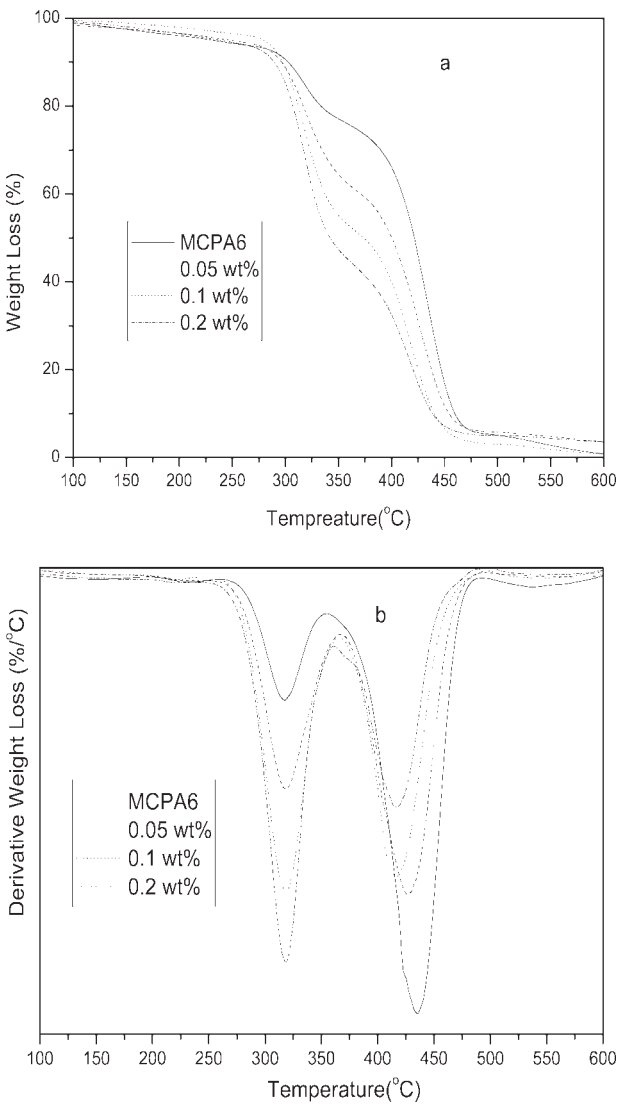

Figure 6 (a) TGA and (b) DTG curves of MCPA6/MWNTs-OH with various amounts of MWNTs-OH under air environment.

TABLE II
Results of TGA Analysis of MCPA6 and MCPA6/MWNTs-OH Composites

MWNTs-OH content (wt %)	$T_{10\ wt\ \%}$ (°C)	$T_{30\ wt\ \%}$ (°C)	$T_{50\ wt\ \%}$ (°C)	$T_{peak\ 2}$ (°C)
0	301	324	420	434
0.05	296	314	398	426
0.10	296	311	372	415
0.20	287	305	340	413

nanocomposites with various amounts of MWNTs-OH under nitrogen and air environment are presented in Figures 5 and 6, respectively. Two-step decomposition behavior can be observed under both nitrogen and air environment from Figures 5 and 6. The onset temperature of degradation (T_{onset}) and the temperatures at maximum mass loss rate (T_{peak}) for the first stage is due to the fact that there are few residue of CL monomer (about 4–6 wt %) in the matrix. This CL residue could induce the decomposition of MCPA6 at a lower temperature. The second stage corresponds to the decomposition of MCPA6.[25] The T_{onset} and T_{peak} for the second stage of the MCPA6/MWNTs-OH are comparable to that of the pristine MCPA6 under nitrogen atmosphere. However a clear decrease in the T_{onset} and T_{peak} for the second stage is found in the MCPA6/MWNTs-OH with respect to pure MCPA6 in an air environment. For a closer analysis, the TGA 10, 30, and 50 wt % loss temperatures and T_{peak} for the second stage (T_{peak2}) in Figure 6 are summarized in Table II. It is found that the 10 wt % and 50 wt % loss temperatures are 14°C and 80°C lower for nanocomposites with 0.2 wt % MWNTs-OH additions than those for neat MCPA6. With increasing the concentration of MWNTs-OH, the T_{peak2} of the nanocomposites decreases. The maximum decrement is 21°C for MCPA6/MWNTs-OH nanocomposites with 0.2 wt % MWNTs-OH.

The low aspect ratios of the as-received MWNTs-OH and the low content of MWNTs-OH in the MCPA6/MWNTs-OH nanocomposites are probably the main reasons for the comparable thermal stability of pure MCPA6 and its nanocomposites under nitrogen environment. On the other hand, it can be noted that there are a few spots with a size of several nanometers on the surface of as-received MWNTs-OH from Figure 2(a), these spots should be attributed to Fe and Ni particles, which were used as catalysts for CVD (chemical vapor deposition) synthesis of MWNTs.[26,27] These two kinds of metal could be easily oxygenated to form metal oxides when being heated in air. It is well known that polymer thermal degradation begins with chain cleavage and radical formation. The metal oxides of Fe (**III**) or Ni (**III**) could easily catalyze the thermal degradation of PA6 as a redox or electron transfer reaction,[28] which led to the poor thermal stability of the MCPA6/MWNTs-OH nanocomposites with respect to pure MCPA6.

CONCLUSIONS

In situ anionic ring opening polymerization has been successfully used to prepare MCPA6/MWNTs-OH nanocomposites as a simple method. The strong hydrogen bond association between MWNTs-OH and the chain facilitated the uniform dispersion of MWNTs-OH in MCPA6 matrix. The well dispersed MWNTs-OH can effectively act as a heterogeneous nucleation of MCPA6. Because of the heterogeneous nucleation of MWNTs-OH, the crystallization temperature and the degree of crystallization of MCPA6 were all increased, whereas the values of ΔT_m and the degree of supercooling were decreased. Although the stability of MCPA6/MWNTs-OH nanocomposites under air environment become worse than that of pure MCPA6, the direct utilization of commercial MWNTs-OH greatly simplified the process for the preparation MCPA6/MWNTs nanocomposites with excellent crystallinity.

References

1. Zhang, W. D.; Shen, L.; Phang, I. Y.; Liu, T. X. Macromolecules 2004, 37, 256.
2. Liu, T. X.; Phang, I. Y.; Shen, L.; Chow, S. Y.; Zhang, W. Macromolecules 2004, 37, 7214.
3. Kim, J. Y.; Kim, S. H. J Polym Sci Part B: Polym Phys 2006, 44, 1062.
4. Bhattacharyya, A. R.; Pötschke, P.; Häuβler, L.; Fischer, D. Macromol Chem Phys 2005, 206, 2084.
5. Lee, H. J.; Oh, S. J. J.; Choi, Y.; Kim, J. W.; Han, J. W. Chem Mater 2005, 17, 5057.
6. Nogales, A.; Broza, G.; Roslaniec, Z.; Schulte, K.; SÿIcs, I.; Hsiao, B. S. Macromolecules 2004, 37, 7669.
7. Hernández, J. J.; García-Gutiérrez, M. C.; Nogales, A.; Rueda, D. R. Polymer 2007, 48, 3286.
8. Broza, G.; Kwiatkowsk, M.; Rosłaniec, Z.; Schultea, K. Polymer 2005, 46, 5860.
9. Zhou, Z.; Wang, S. F.; Lu, L.; Zhang, Y. Compos Sci Technol 2007, 67, 1861.
10. Rasheed, A.; Dadmun, M. D.; Ivanov, I.; Britt, P. F.; Geohegan, D. B. Chem Mater 2006, 18, 3513.
11. Krul, L. P.; Volozhyn, A. I.; Belov, D. A.; Poloiko, N. A.; Artushkevich, A. S. Biomol Eng 2007, 24, 93.
12. Jose, M. V.; Steinert, B. W.; Thomas, V.; Dean, D. R. Polymer 2007, 48, 1096.
13. Wu, H. L.; Wang, C. H.; Ma, C. C. M.; Chiu, Y. C. Compos Sci Technol 2007, 67, 1854.
14. Yuen, S. M.; Ma, C. C. M.; Lin, Y. Y.; Kuan, H. C. Compos Sci Technol 2007, 67, 2564.
15. Wang, S. F.; Shen, L.; Zhang, W. D.; Tong, Y. J. Biomacromolecules 2005, 6, 3067.
16. Mitchell, C. A.; Bahr, J. L.; Arepalli, S.; Tour, J. M.; Krishnamoorti, R. Macromolecules 2002, 35, 8825.
17. Sung, J. H.; Kim, H. S.; Jin, H. J.; Choi, H. J.; Chin, I. J. Macromolecules 2004, 37, 9899.

18. Sabba, Y.; Thomas, E. L. Macromolecules 2004, 37, 4815.
19. Wang, Y.; Deng, J.; Wang, K.; Zhang, Q.; Fu, Q. J Appl Polym Sci 2007, 104, 3695.
20. Saeed, K.; Park, S. Y. J Appl Polym Sci 2007, 106, 3729.
21. Gao, B.; Zhao, B.; Itkis, M. E.; Bekyarova, E.; Hu, H.; Kranak, V. J Am Chem Soc 2006, 128, 7492.
22. Zhao, C. G.; Hua, G. J.; Justiceb, R. Polymer 2005, 46, 5125.
23. Sun, L.; Yang, J. T.; Lin, G. Y.; Zhong, M. Q. Mater Lett 2007, 61, 3963.
24. Wan, T.; Chen, L.; Chua, Y. C.; Lu, X. H. J Appl Polym Sci 2004, 94, 1381.
25. Liu, A. D.; Xie, T. X.; Yang, G. S. Macromol Chem Phys 2006, 207, 701.
26. Liang, Q.; Gao, L. Z.; Li, Q.; Tang, S. H.; Liu, B. C.; Yu, Z. L. Carbon 2001, 39, 897.
27. Liu, B. C.; Tang, S. H.; Yu, Z. L.; Zhang, B. L. Chem Phys Lett 2002, 357, 297.
28. Gupta, M. C.; Jais, A. T. Thermochim Acta 1993, 230, 155.